JOURNAL OF GUIDANCE, CONTROL, AND DYNAMICS
Vol. 16, No. 1, January-February 1993

Application of Quantitative Feedback Theory to a Class of Missiles

Daniel G. Benshabat* and Yossi Chait†
University of Massachusetts, Amherst, Massachusetts 01003

A control design problem is investigated for a class of missiles that exhibits unstable and nonminimum phase behavior over a large flight envelope. Traditional control design for this class consists of a set of controllers, designed at different operating points within the flight envelope, which are implemented using the gain-scheduling method. The quantitative feedback theory is proposed for this class to overcome certain control design and implementation difficulties related to gain scheduling. In particular, the advantages in using quantitative feedback theory are that 1) it is possible to investigate the feasibility of fixed controllers for the whole flight envelope, and 2) it reveals tradeoffs between the size of flight envelope, controller complexity, and closed-loop specifications. These advantages are illustrated using a control design for the longitudinal dynamics of a Vanguard missile.

Nomenclature

a_x = longitudinal acceleration
a_z = vertical acceleration
C_{m_q} = aerodynamic pitch damping
C_{m_α} = pitching moment coefficient slope with angle of attack
C_{m_δ} = pitching moment coefficient slope with fin deflection
C_{z_α} = lift force coefficient in z direction with α
C_{z_δ} = fin force coefficient in z direction with γ
d = reference missile radius
h = flight altitude
I_y = moment of inertia about the y direction
M = Mach number
m = mass of missile
q = dynamic pressure
S = reference missile area
U = total velocity
z = linear position in z direction
α = angle of attack
γ = flight-path angle
δ = fin angle
δ_c = fin-angle command
θ = pitch angle
$\dot{\theta}$ = pitch angular velocity
$\ddot{\theta}$ = pitch angular acceleration
τ = servo time constant

I. Introduction

A CHALLENGING task for control engineers is the design of a missile's autopilot to achieve desired robust stability and robust performance over a large flight envelope (defined as altitude vs Mach number). This task can become particularly difficult if the missile is tail controlled, due to its nonminimum phase (nmp) dynamic behavior. It is well known that nmp zeros restrict the achievable performance of the closed-loop system.[1,2] Hence, it is reasonable to expect that certain performance specifications are unattainable for this class of missile.

A traditional control design method employed for such missiles operating over a large flight envelope is gain scheduling.[3,4] In this method, the missile's nonlinear dynamics are linearized about a set of operating points within the flight envelope, which results in a set of transfer functions. Subsequently, separate controllers are found for each transfer function that achieve the closed-loop objectives. Implementation of this design requires on-line updating of the controllers as the missile travels from one operating point to another (i.e., gain scheduling). Naturally, to simplify the implementation, maintaining a fixed topology (structure) of all of these controllers is desired. Unfortunately, it is not simple to determine whether a controller with constant topology exists or can be derived over the whole flight envelope. Even if a constant topology controller can be found over the whole flight envelope, its implementation at a large number of operating points may place great demands on available on-board computing capacity. And updating of controller parameters will introduce undesired inputs to the missile's dynamics that can cause unpredictable behavior during and after updating. Therefore, prior to implementation of gain-scheduling controllers, extensive simulations are required to verify the actual response of the closed-loop system.

One alternative method for control design for this class of problems, which possibly can alleviate the abovementioned difficulties, is the quantitative feedback theory (QFT).[5,6] The QFT is a frequency domain method for control design of systems with plant uncertainty and performance specifications. In this method, closed-loop specifications are first mapped into appropriate bounds on a nominal loop transmission function, followed by shaping of a nominal loop transfer function. In the context of missile control design, variations in the missile's linearized dynamics over the flight envelope will be defined as plant uncertainty. Given this uncertainty definition and the desired performance specifications, QFT can be useful for several reasons: 1) It can be used to find a fixed, time-invariant controller over the whole flight envelope (where it is possible) and thus simplify the implementation, and 2) it reveals the tradeoffs between the size of flight envelope, controller complexity, and specifications. The latter reason is particularly important because the missile's parameters are often changed during the development stage, rendering the control design process highly iterative. To illustrate the effectiveness of QFT for robust control design for a large class of missiles (e.g., ballistic, surface-to-air, and air-to-surface), it was applied to a ballistic-type missile (Vanguard) that is inherently unstable and nmp over the whole flight envelope.

This paper is organized as follows. The missile's linearized longitudinal dynamics are described in Sec. II. The control

Received May 17, 1991; revision received Nov. 2, 1991; accepted for publication April 29, 1992.

*Graduate Research Assistant, Department of Mechanical Engineering.
†Assistant Professor, Department of Mechanical Engineering.

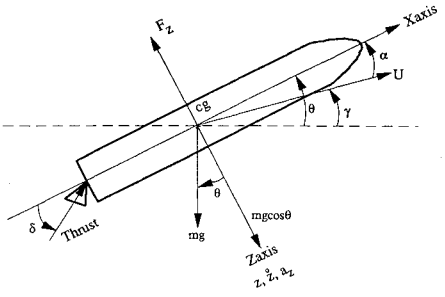

Fig. 1 Schematic of a Vanguard missile.

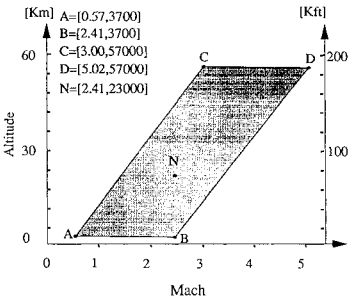

Fig. 2 Flight envelope.

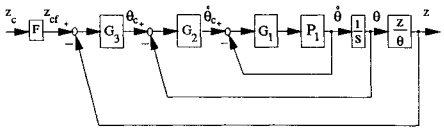

Fig. 3 Block diagram of the control system.

design problem is stated in Sec. III. A QFT control design is presented in Sec. IV along with relevant details. Finally, in Sec. V we propose an improved design that includes both QFT and scheduling.

II. Longitudinal Dynamics

The equations of motion for the missile's dynamics are nonlinear (Fig. 1). However, by using standard assumptions in this field,[7] they are linearized about an operating point. This linearization results in the following three transfer functions for the longitudinal dynamics. The transfer function relating the fin angle to the pitch angular velocity of the linearized dynamics is given by

$$\frac{\dot{\theta}}{\delta}(s) = K_\theta \frac{(s+z_\theta)}{(s+p_s)(s-p_u)} \tag{1}$$

The transfer function relating the fin angle to the linear vertical acceleration is given by

$$\frac{a_z}{\delta}(s) = K_a \frac{(s+z_s)(s-z_u)}{(s+p_s)(s-p_u)} \tag{2}$$

The transfer function relating the angular pitch position to the linear position is given by

$$\frac{z}{\theta}(s) = K_z \frac{(s+z_s)(s-z_u)}{s(s+z_\theta)} \tag{3}$$

The details of the foregoing transfer functions are given in the Appendix. It is common to approximate the servo transfer function, within the performance bandwidth, with a first-order type[7]

$$G_s(s) = \frac{\delta}{\delta_c}(s) = \frac{1}{s/\tau+1} \tag{4}$$

III. Problem Statement

Consider a Vanguard missile described by Eqs. (1-4) operating at a flight envelope of dynamic pressures q between 240 and 265,000 N/m^2 (Fig. 2). Note that the transfer functions (1-3) are unstable, nmp and unstable, and nmp, respectively, over this flight envelope. To achieve the performance specifications, a typical feedback control configuration used in this class of problems is shown in Fig. 3, where the transfer function $P_1(s)$ is given by

$$P_1(s) = \frac{\delta}{\delta_c}(s)\frac{\dot{\theta}}{\delta}(s) \tag{5}$$

For illustration purposes only, let the following describe the closed-loop objectives that must be met over the whole flight envelope (Fig. 2):

1) Stability
2) Performance at each loop:
   a) The frequency response magnitude of the angular velocity transfer function $\dot{\theta}/\dot{\theta}_c(j\omega)$ must lie within its bounds (Fig. 4) up to $\omega = 100$ rad/s.
   b) The frequency response magnitude of the angular position transfer function $\theta/\theta_c(j\omega)$ must lie within its bounds (Fig. 5) up to $\omega = 10$ rad/s.
   c) The frequency response magnitude of the linear position transfer function $z/z_c(j\omega)$ must lie within its bounds (Fig. 6) up to $\omega = 1$ rad/s.

The control problem is to find the controllers $G_1(s)$, $G_2(s)$, $G_3(s)$, and the prefilter $F(s)$, such that the closed-loop system satisfies the foregoing objectives. Because these objectives must be met over the whole flight envelope, this problem is referred to as a *robust* control design problem.

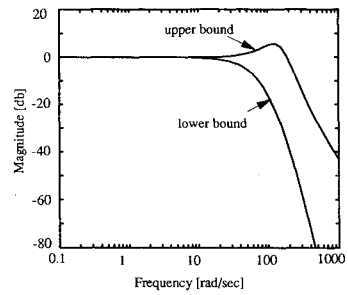

Fig. 4 Frequency domain tracking bounds for first loop, $\dot{\theta}/\dot{\theta}_c$.

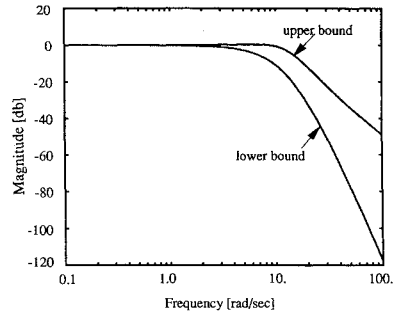

Fig. 5 Frequency domain tracking bounds for second loop, θ/θ_c.

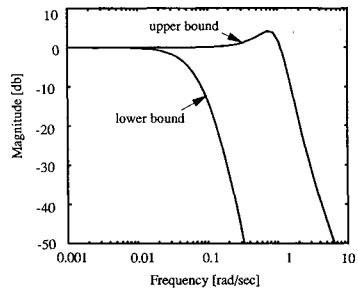

Fig. 6 Frequency domain tracking bounds for third loop, z/z_c.

IV. QFT Control Design

The feedback control system shown in Fig. 3 with three feedback loops requires the design of three compensators $G_1(s)$, $G_2(s)$, and $G_3(s)$, and a prefilter $F(s)$. In general, this design can be accomplished using two approaches: 1) a sequential design from the outermost loop toward the innermost loop, where at each step the design assumes that all inner loops are equal to unity[8] (i.e., infinite bandwidth), and 2) a sequential design from the innermost loop toward the outermost loop. The second approach requires no assumptions regarding the bandwidths of the other loops. Our design employs the second approach because the missile is unstable [Eq. (1)] and nmp [Eq. (3)]. If the design was to start from the outer loop and proceed inward, the inner loop design would then have to cope with an unstable and nmp plant that has large uncertainty. Such a combination of an unstable pole and a nmp zero would further complicate the control design problem. In contrast, the second approach avoids this problem since the outer loop design (last step) has to cope only with an uncertain nmp plant. Therefore, our design will start wth the $\dot{\theta}/\dot{\theta}_c(s)$ loop and end with the $z/z_c(s)$ loop.

Regardless of the specific design approach, an exact definition of the plant template must first be established. The collection of all frequency responses, at each fixed frequency, corresponding to the selected operating points in the flight envelope is referred to in the QFT literature as a *template* (examples of templates are shown in Fig. 7). Because any flight envelope consists of an infinite number of operating points, one must grid the envelope. An appropriate grid of the flight envelope can be defined using the engineer's understanding of the missile's dynamics (as done in practice). Naturally, such a procedure cannot guarantee that the design objectives will actually be satisfied over the whole flight envelope. Nevertheless, for practical design purposes this procedure is sufficient. In the example considered in this paper, 982 operating points were used within the flight envelope of Fig. 2 to form the templates. These were chosen after considering the behavior of the templates as a function of operating points.

Let us now briefly review the QFT control design that involves two separate steps. The first step translates robust stability and robust performance specifications placed on an uncertain plant into certain domains in the complex plane (or Nichols chart). A nominal loop transmission is then designed such that it lies within these domains at various frequencies (i.e., loop shaping). These domains are referred to in the literature as QFT *bounds*.[5] These bounds can be derived using graphical methods (e.g., see Ref. 9) or computer searches. However, it has been shown recently that a closed-form map from the problem statement to the corresponding QFT bounds can be derived for multiple-input/single-output and multiple-input/output continuous systems, and multiple-input/single-output sampled-data systems.[10-12] Let us proceed with the actual control design for each loop.[13]

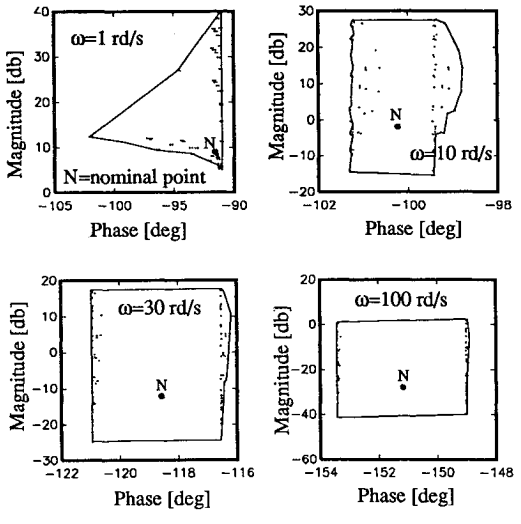

Fig. 7 Templates of $P_1(s)$ used in the first loop design.

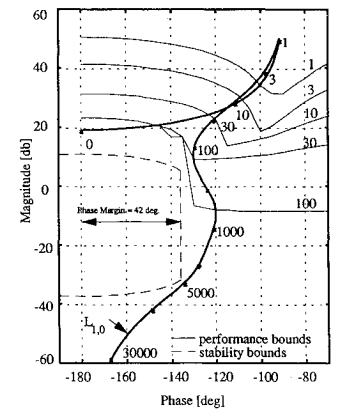

Fig. 8 QFT bounds and nominal loop for first loop, $L_{1,0}(s) = G_1(s)P_{1,0}(s)$.

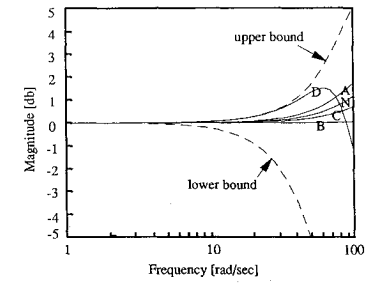

Fig. 9 Closed-loop robust performance vs specification in the first loop.

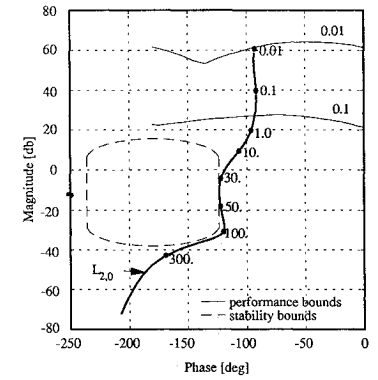

Fig. 10 QFT bounds and nominal loop for second loop, $L_{2,0}(s) = G_2(s)P_{2,0}(s)$.

First Loop

The transfer function of the inner loop has one unstable pole p_u and is given by

$$P_1(s) = G_s(s)\frac{\dot{\theta}}{\delta}(s) = K_\theta \frac{(s+z_\theta)}{(s/\tau+1)(s+p_s)(s-p_u)} \tag{6}$$

The nominal operating point was arbitrarily chosen at a 23,000-m (76,000-ft) altitude and Mach number of 2.41. Note that the choice of nominal point has no effect whatsoever on any aspect of the QFT control design. The plant evaluated at the nominal operating point is referred to as the nominal plant $P_{1,0}(s)$. As expected, due to the large flight envelope, the variations in the gain, zero, and pole in Eq. (6) are *extremely* large: $K_\theta \in [-1.25, -226.0]$, $z_\theta \in [0.0003, 0.21]$, $p_u \in [0.2, 5.8]$, and $p_s \in [0.2, 5.4]$. Moreover, a parametric uncertainty in the servo

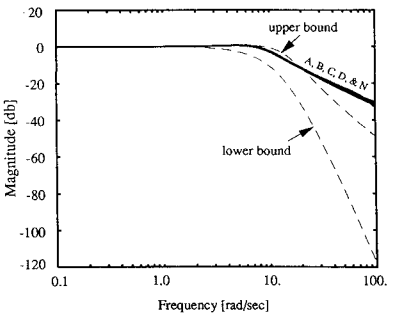

Fig. 11 Closed-loop robust performance vs specification in the second loop.

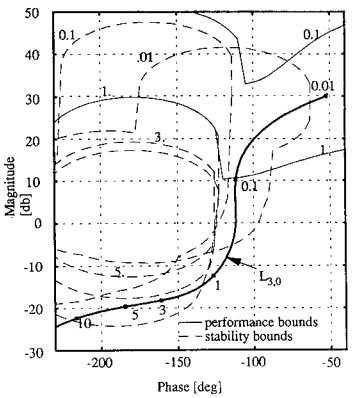

Fig. 12 QFT bounds and nominal loop for third loop, $L_{3,0}(s) = G_3(s)P_{3,0}(s)$.

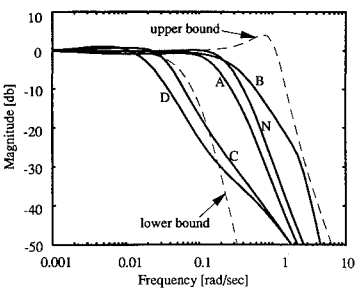

Fig. 13 Closed-loop robust performance vs specification in the third loop.

time constant was also taken into consideration in the design, $\tau \in [50, 60]$.

A QFT design was carried out at several frequencies within the performance bandwidth (i.e., up to 100 rad/s), and several templates used in the design are shown in Fig. 7. The robust stability and robust performance bounds on the nominal loop transmission $L_{1,0}(s) = G_1(s)P_{1,0}(s)$ were computed and are shown in Fig. 8. The nominal loop transmission shown in Fig. 8 has the compensator

$$G_1(s) = -100\,\frac{(s/220+1)(s/2100+1)}{(s/1200+1)(s/7600+1)} \tag{7}$$

Note that because the phase of the transfer function in Eq. (1) at $s=0$ is -180 deg, a negative gain in $G_1(s)$ was needed to achieve an in-phase steady-state response. The response of the uncertain closed-loop transfer function $T_1(s) = L_1(s)/[1+L_1(s)]$ was checked at several operating points, $[A, B, C, D, N]$ (shown in Fig. 2). Indeed, all of the objectives (robust stability and robust performance) in this loop were achieved by the QFT design using a fixed, time-invariant controller over the whole envelope (Fig. 9).

Second Loop

The open-loop transfer function $P_2(s)$ in the second loop (angular position) is obtained by cascading an integrator and the closed-loop transfer function of the first loop $T_1(s) = L_1(s)/[1+L_1(s)]$. Therefore, the open-loop transfer function of the second loop is given by

$$P_2(s) = T_1(s)(1/s) \tag{8}$$

Although not required by the QFT design procedure, it is convenient to choose the nominal operating point in the first loop as the nominal point in the second loop. The nominal plant is denoted by $P_{2,0}(s)$. The robust stability and robust performance bounds on the nominal loop transmission $L_{2,0}(s)G(s)P_{2,0}(s)$ are shown in Fig. 10, where the compensator is given by

$$G_2(s) = 9.8\,\frac{(s/15.7+1)(s/67+1)}{(s/6.4+1)(s/37.4+1)} \tag{9}$$

The performance of the uncertain closed-loop transfer function $T_2(s) = L_2(s)/[1+L_2(s)]$ was checked at the same operating points used before, i.e., $[A, B, C, D, N]$. Again, the QFT design meets all specifications using a fixed, time-invariant

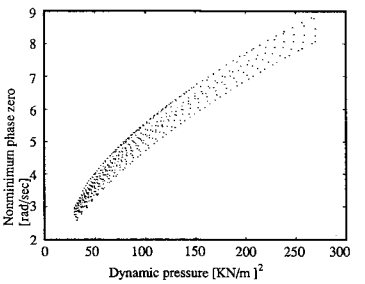

Fig. 14 Nonminimum phase zero location z_u vs dynamic pressure q.

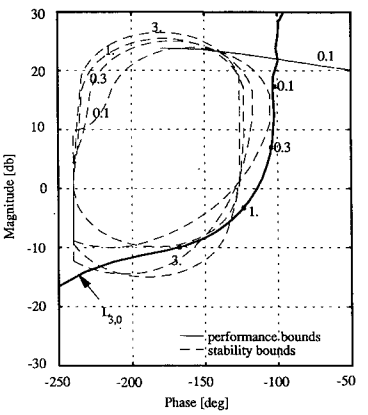

Fig. 15 QFT bounds nominal loop for the redesigned third loop, $L_{3,0}(s) = G_3(s)P_{3,0}(s)$.

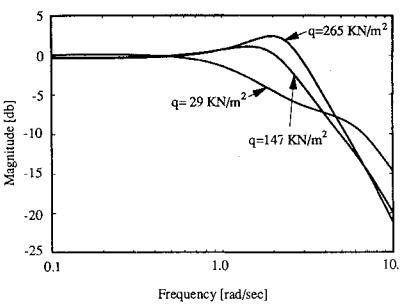

Fig. 16 Closed-loop robust performance vs specification in the improved third loop.

controller over the whole flight envelope (Fig. 11). Note that since the uncertainty in $T_1(s)$ is sufficiently small and the integrator further reduces this uncertainty at low frequencies, the real design problem in this loop was merely to guarantee robust stability.

Third Loop

The transfer function for the outer loop (linear position) is obtained by cascading the transfer function in Eq. (3) and the closed-loop transfer function of the second loop $T_2(s) = L_2(s)/[1+L_2(s)]$. Therefore, the open-loop transfer function P_3 of the third loop is given by

$$P_3(s) = T_2(s)\frac{K_z(s+z_s)(s-z_u)}{s(s+z_\theta)} \tag{10}$$

The nominal operating point is again the same one used in the first and second loops. The nominal plant is denoted by $P_{3,0}(s)$. Because of the large flight envelope, the variations in the gain, zero, and pole variations in Eq. (10) are *very large*: $K_z \in [-7.15, -10.25]$, $z_u \in [0.33, 8.9]$, and $z_s \in [0.33, 8.6]$. However, unlike the situation in the preceding loops, there is an inherent control design limitation in the third loop due to the nmp zero. It is well known that the achievable bandwidth of a system with a nmp zero is limited.[1,2] Therefore, the high bandwidth required to achieve the desired reduction in the variations of the third loop's closed-loop transfer function may not be feasible. Indeed, this was found to be the case here, and the third loop's bandwidth was limited to 0.2 rad/s [approximated by the formula $(1-\alpha)\min(z_u)$, $\alpha<1$], which is below the specifications (Fig. 6). Of course, the prefilter $F(s)$ can improve the speed of the tracking response, but it cannot reduce the variations in the closed-loop transfer function. In other words, in this problem it is impossible to place the third loop's transfer function with its frequency-response performance bounds.

Nevertheless to complete the design we attempted to increase the bandwidth as much as possible and obtained a compensator $G_3(s)$ and prefilter F for which the QFT robust stability bounds and nominal loop transmission $L_{3,0}(s) = G_3(s)P_{3,0}(s)$ are shown in Fig. 12. The compensator and prefilter are described by

$$G_3(s) = 4.10^{-5}\frac{(s/0.0027+1)(s/0.11+1)(s/1.08+1)}{(s/0.035+1)(s/0.83+1)(s/8.33+1)} \tag{11}$$

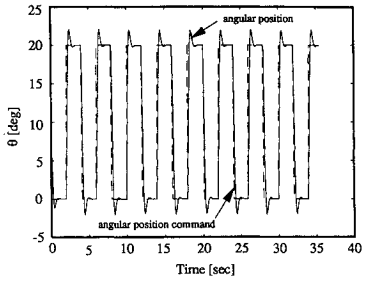

Fig. 17 Time response of pitch angle θ to a square wave command θ_c.

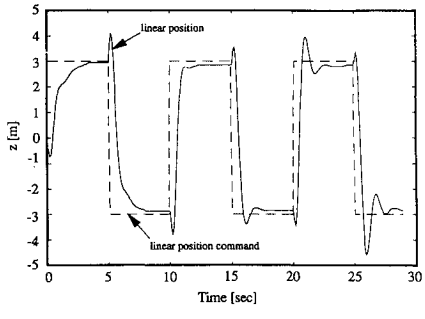

Fig. 18 Time response of linear position z to a square wave command z_c.

$$F(s) = \frac{(2.5)^2}{(s+2.5)^2} \tag{12}$$

The uncertain closed-loop transfer function $T_3(s) = F(s)L_3(s)/[1+L_3(s)]$ was simulated at the same operating points $[A, B, C, D, N]$, and clearly does not meet its specifications (Fig. 13).

Although we have just demonstrated how QFT can be very useful for the design of fixed, time-invariant controllers for this class of problems, the limitations of time-invariant controllers were also made evident. Therefore, we are naturally led to propose the following improvement in control design for this class of problems.

V. Improved Control Design

A linear, time-invariant controller (obtained using QFT or any other linear robust control design technique) cannot be found to achieve the performance specifications in the third loop, due to the location of the nmp zero. Therefore, to meet the specifications in the third loop using a fixed topology controller, we propose to consider both QFT and scheduling as a combined design tool.

As a preliminary step, we decided to investigate whether it is reasonable to insist that the third loop's performance be met over the whole flight envelope. From previous design efforts, it is known that if the nmp zero is bounded below by 2.5 rad/s, a bandwidth of approximately 1.5 rad/s may be feasible (compared with only 0.2 rad/s with the full envelope). By using the relation between the location of the nmp zero and the dynamic pressure, a nmp zero with a lower bound of 2.5 can be made possible if the dynamic pressure is bounded below by 29,000 N/m^2 (Fig. 14). This reduction in the size of the envelope can be justified because the truncated lower range of dynamic pressure (between 240 and 29,000 N/m^2) corresponds to very high altitudes or very low Mach numbers. At these conditions it is not physically sensible to demand a fast response.

To avoid implementation problems due to scheduling, we decided to allow for only one parameter of the controller to vary with the flight envelope. For an engineer well versed with the dynamics of the missile, the choice of this parameter is very natural. Using Eq. (3), the steady-state gain of the third loop's transfer function K_{dc} is given by

$$K_{dc} = K_z\frac{z_s z_u}{z_\theta} \tag{13}$$

Using the relationships for K_z, z_s, z_u, and z_θ given in the Appendix, one can conclude that the steady-state gain of the third loop is also equal to the missile's total velocity

$$K_{dc} = U \tag{14}$$

Now assume that during the control design the value of this gain remains fixed. This will result in a template with a reduced size and, subsequently, less conservative bounds compared with those for an uncertain gain. Therefore, we propose to perform a QFT design for a plant with a certain steady-state gain and in implementation update the gain of the controller as a function of the missile's total velocity, as in Eq. (14). Indeed, by using this improvement, the robust stability bounds become less conservative (Fig. 15) compared with those for an uncertain gain (Fig. 12). Now, with the decreasing stability bounds, a third loop can be derived with a larger bandwidth. The new single compensator $G_3(s)$ that achieves the specifications for the third loop is given by

$$G_3(s) = K_3\frac{(s/0.085+1)(s/2.8+1)}{(s/1.88+1)(s/3.8+1)} \tag{15}$$

where

$$K_3 = 0.9/U \tag{16}$$

The frequency domain responses of the improved third loop design (Fig. 16) verify the improvement in the closed-loop system's bandwidth.

Naturally, this proposed scheduling relies heavily on the accuracy of the measurement of the missile's total velocity. Fortunately, it is possible to measure the total velocity using accelerometers and rate gyros, already used for feedback, and navigation algorithms[14] (strapdown). Any sensor and algorithm errors can be considered as uncertainty in the model.

Time Domain Simulations

The system was tested in a three-degree-of-freedom nonlinear simulation of the longitudinal dynamics shown in the Appendix. The parameters of the missile's nonlinear dynamics were allowed to vary with time as the missile traveled around the envelope. To test the closed-loop behavior over the whole envelope, a square wave was chosen as the (somewhat nontraditional) input signal. The transient response of the angular (second) loop (Fig. 17) indicated that the performance occurred as expected. A similar test for linear position (third) loop (Fig. 18) with a square wave command input over the reduced envelope (defined earlier) verified that the proposed design improvement resulted in a successful design. In both Figs. 17 and 18, calculations showed that the command inputs caused the missile to travel over the whole range of dynamic pressure in the envelope.

VI. Summary

The problem of controller design was investigated for an unstable and nmp Vanguard missile traveling over a large flight envelope. It was found that, in spite of the large flight envelope, quantitative feedback theory can be used to design fixed, time-invariant controllers to achieve robust stability and robust performance. It was shown that significant improvements in the performances of the linear position loop with the nmp zero can be achieved by a combination of a physically motivated reduction of the flight envelope, quantitative feedback theory design, and scheduling of the steady-state gain.

References

[1]Horowitz, I., "Design of Feedback Systems with Non-Minimum-Phase Unstable Plants," *International Journal of Systems Science,* Vol. 10, No. 9, pp. 1025–1040.

[2]Fruedenberg, J. S., and Looze, D. P., *Frequency Domain Properties of Scalar and Multivariable Feedback Systems,* Lecture Notes in Control and Information Science, 109, Springer-Verlag, New York, 1988.

[3]Åström, K. J., and Wittenmark, B., *Adaptive Control,* Addison-Wesley, Reading, MA, 1989.

[4]Stein, G., "Adaptive Flight Control—A Pragmatic View," *Applications of Adaptive Control,* edited by K. S. Narenda and R. V. Monopoli, Academic Press, New York, 1980.

[5]Horowitz, I., and Sidi, M. "Synthesis of Linear Systems with Large Plant Uncertainty for Prescribed Time-Domain Tolerances," *International Journal of Control,* Vol. 16, No. 2, 1972, pp. 287–309.

[6]Horowitz, I. M., *Synthesis of Feedback Systems,* Academic Press, New York, 1963.

[7]Blakelock, J. H., *Automatic Control of Aircraft and Missiles,* Wiley, New York, 1965.

[8]Horowitz, I., and Sidi, M., "Synthesis of Cascaded Multiple-Loop Feedback Systems with Large Plant Parameters Ignorance," *Automatica,* Vol. 9, 1973, pp. 589–600.

[9]D'Azzo, J. J., and Houpis, C. H., *Linear Control System Analysis and Design,* 3rd ed., McGraw-Hill, New York, 1988, Chap. 21.

[10]Chait, Y., and Yaniv, O., "Multi-Input/Single-Output Computer Aided Control Design Using the Quantitative Feedback Theory," *International Journal of Robust and Nonlinear Control* (in press).

[11]Yaniv, O., and Chait, Y., "A Simplified Multi-Input/Output Formulation for the Quantitative Feedback Theory," *ASME Journal of Dynamic Systems, Measurements, and Control* (to be published).

[12]Yaniv, O., and Chait, Y., "Direct Robust Control of Uncertain Sampled-Data Systems Using the Quantitative Feedback Theory," *Proceedings of the American Control Conference* (Boston, MA), 1991, pp. 1987–1988; also *Automatica* (to be published).

[13]Benshabat, D. G., "Robust Control Design for a Class of Missiles with Large Flight Envelope," M.S. Thesis, Dept. of Mechanical Engineering, Univ. of Massachusetts, Amherst, MA, 1991.

[14]Offereins, R. P., "Methods for Strap-Down Attitude Estimation and Navigation with Accelerometers," *Guidance and Control Panel Symposium,* (Ottawa, Ontario, Canada), AGARD, May 1979.

Appendix

The equations of motion for the missile longitudinal dynamics are as follows:

$$I_y\ddot{\theta} = Sqd\left(C_{m_\alpha}\alpha + C_{m_\delta}\delta + \frac{d}{2u}C_{m_q}\dot{\theta}\right) \qquad ma_z = Sq(C_{z_\alpha}\alpha + C_{z_\delta}\delta) + mg\cos(\theta) \qquad ma_x = \text{thrust}\cos(\delta) - mg\sin(\theta)$$

where $\theta = \alpha + \gamma$ and $a_z \cong -U\dot{\gamma}$.

By using linearization of the missile longitudinal plane equations, the transfer functions of the fin angle to angular velocity [Eq. (1)], fin angle to acceleration [Eq. (2)], and angular position to linear position [Eq. (3)] can be derived. The specific parameters in Eqs. (1–3) are

$$K_\theta = \frac{Sqd}{I_y}C_{m_\delta}$$

$$z_\theta = \frac{Sq}{mU}\left(\frac{C_{z_\delta}}{C_{m_\delta}}C_{m_\alpha} - C_{z_\alpha}\right)$$

$$p_u = Sq\left[\frac{d}{4U}C_{\tilde{m}_q} - \frac{C_{m_\alpha}}{2mU} + \sqrt{\left(\frac{d}{4U}C_{\tilde{m}_q} - \frac{C_{m_\alpha}}{2mU}\right)^2 + \frac{d}{mUI_y}\left(\frac{mU}{Sq}C_{m_\alpha} - C_{\tilde{m}_q}C_{z_\alpha}\right)}\right]$$

$$p_s = Sq\left[\frac{d}{4U}C_{\tilde{m}_q} - \frac{C_{m_\alpha}}{2mU} - \sqrt{\left(\frac{d}{4U}C_{\tilde{m}_q} - \frac{C_{m_\alpha}}{2mU}\right)^2 + \frac{d}{mUI_y}\left(\frac{mU}{Sq}C_{m_\alpha} - C_{\tilde{m}_q}C_{z_\alpha}\right)}\right]$$

$$K_z = -\frac{I_y}{dm}\frac{C_{z_\delta}}{C_{m_\delta}}$$

$$z_u = \frac{1}{2}\left(C_{\tilde{m}_q}\frac{Sqd}{I_y}\right) + \sqrt{\frac{1}{4}\left(C_{\tilde{m}_q}\frac{Sqd}{I_y}\right)^2 + \left(C_{m_\alpha} - \frac{C_{\tilde{m}_\delta}}{C_{z_\delta}}C_{z_\alpha}\right)\frac{Sqd}{I_y}}$$

$$z_s = -\frac{1}{2}\left(C_{\tilde{m}_q}\frac{Sqd}{I_y}\right) + \sqrt{\frac{1}{4}\left(C_{\tilde{m}_q}\frac{Sqd}{I_y}\right)^2 + \left(C_{m_\alpha} - \frac{C_{\tilde{m}_\delta}}{C_{z_\delta}}C_{z_\alpha}\right)\frac{Sqd}{I_y}}$$

$$C_{\tilde{m}_q} = \frac{d}{2U}C_{m_q}$$